



UNIVERSITY OF LEEDS

This is a repository copy of *Mixed protein-polysaccharide interfacial layers: Effect of polysaccharide charge distribution*.

White Rose Research Online URL for this paper:
<http://eprints.whiterose.ac.uk/85093/>

Article:

Ettelaie, R orcid.org/0000-0002-6970-4650, Akinshina, A and Maurer, S (2012) Mixed protein-polysaccharide interfacial layers: Effect of polysaccharide charge distribution. *Soft Matter*, 8 (29). pp. 7582-7597. ISSN 1744-683X

<https://doi.org/10.1039/c2sm25803j>

© 2012, Royal Society of Chemistry. This is an author produced version of a paper *Soft Matter*. Uploaded in accordance with the publisher's self-archiving policy.

Reuse

Unless indicated otherwise, fulltext items are protected by copyright with all rights reserved. The copyright exception in section 29 of the Copyright, Designs and Patents Act 1988 allows the making of a single copy solely for the purpose of non-commercial research or private study within the limits of fair dealing. The publisher or other rights-holder may allow further reproduction and re-use of this version - refer to the White Rose Research Online record for this item. Where records identify the publisher as the copyright holder, users can verify any specific terms of use on the publisher's website.

Takedown

If you consider content in White Rose Research Online to be in breach of UK law, please notify us by emailing eprints@whiterose.ac.uk including the URL of the record and the reason for the withdrawal request.



eprints@whiterose.ac.uk
<https://eprints.whiterose.ac.uk/>

Cite this: DOI: 10.1039/c0xx00000x

www.rsc.org/xxxxxx

ARTICLE TYPE

Mixed Protein–Polysaccharide Interfacial Layers: Effect of Polysaccharide Charge Distribution

Rammile Ettelaie,* Anna Akinshina and Sania Maurer

Received (in XXX, XXX) Xth XXXXXXXXXX 200X, Accepted Xth XXXXXXXXXX 200X

DOI: 10.1039/b000000x

ABSTRACT The influence of the polysaccharide charge distribution on the structure, thickness, and charge reversal of the interfacial layers, formed by adsorbed positively charged protein and oppositely charged polysaccharide, has been investigated using lattice-based self-consistent field (SCF) approach. We compare the adsorption behaviour of a uniformly charged polysaccharide model with that consisting of a short and a long block carrying different charge densities. For homogeneously charged polysaccharide we observe a resulting interfacial layer that is closer to a mixed protein + polysaccharide film, rather than a multi-layer. We also find that the maximum adsorption of polysaccharide occurs at an optimal value of its charge, above and below which the adsorbed amount decreases. In contrast, for heterogeneously charged chains, as their charge is increasingly located on the shorter block, a much thicker interfacial layer results. In such cases the weakly charged longer blocks extend well away from the surface into the solution. The interfacial film begins to resemble a multilayer with a primary protein and a distinct secondary polysaccharide layer. When the weakly charged long blocks still have a sufficient amount of negative charge, we also observe a reversal of the sign of surface potential from positive to a negative value. Our SCF calculated values for the reversed surface potential are of the order of -25 mV, in good agreement with several experimental results involving ζ -potential measurements on particles covered with such protein + polysaccharide films.

1 Introduction

Layer-by-layer (LBL) deposition method involves fabrication of multi-layered films, by consecutive adsorption of alternating charged polyelectrolytes onto a substrate or at an interface^{1,2}. The process is driven by the attractive electrostatic interactions between the polyelectrolyte and the oppositely charged surface. At each stage of the deposition, the adsorbed polyelectrolyte causes a reversal of the charge of the substrate. This then allows for the next layer of polyelectrolyte, with a charge opposite to that of previous layer, to be adsorbed. Normally, there is also a rinsing step before the substrate is dipped into the solution of the appropriate polyelectrolyte, during each stage of the process^{1,3}. Due to its inherent simplicity, the extensive choice of polyelectrolytes and the relatively large and precise number of layers that can be deposited, the technique has been exploited as a potentially useful method in many varied areas of technology, often involving nano-fabrication. Furthermore, the method has been extended to include deposition of charged nano-particles⁴⁻⁶ and even living viruses⁷, either in combination with a polyelectrolyte, or on their own, in formation of multi-layers.

To mention a few possible applications of LBL, Hyde et al.⁸ adsorbed alternative layers of poly(allylamine hydrochloride) and poly(sodium 4-styrene sulfonate) onto cotton fibres, with a view to control the surface selectivity and permeability of the fibres

and thus develop functional textiles. They reported depositing as many as 20 individual layers⁸ onto the surface of such substrates. Even larger numbers, up to 100, alternate layers of polyaniline and poly(styrene sulfonate) were laid on quartz substrates using a novel automated in flow deposition apparatus.⁹ The technique has also been used in the design of more efficient fuel cells, where membranes with high proton conductivity but also good methanol blocking properties, needed in such cells, were fabricated using LBL deposition method¹⁰. LBL based techniques have similarly been used in the development of integrated optics¹¹, in the fabrication of targeted wound dressing materials¹², production of high conductivity¹³ and free standing highly ductile biocompatible films¹⁴, design of ultrafiltration membranes¹⁵ and engineering of superior amperometric bio-sensors.^{16,17} The advances in applying LBL technique to synthesis of superhydrophobic or superhydrophilic surfaces were reviewed by Jaber and Schlenoff.¹⁸

Other notable fields that have also been focus of much recent research activity in self assembly of polyelectrolyte multi-layers are pharmaceuticals, nutraceuticals and food systems. Much of the interest in pharmaceuticals arises from the potential that the multi-layers offer in design of controlled release vehicles and targeted delivery of drugs.¹⁹ Similar considerations also apply to nutraceuticals, where the controlled release of flavour ingredients or functional nutrients, either during mastication or within certain part of digestive systems, may be required. In the past, LBL

technique is often been used in this context to form microcapsules and to load these with the active material.¹⁹ The microcapsule contains the drug which is released as it diffuses across the multi-layer film surrounding the capsule. Thus, by varying the nature and the number of deposited layers, a better degree of control over the release profile of drugs from such microcapsules can be achieved. Similarly, in the burst type release microcapsules, the mechanical properties of multi-layers are generally easier to tune, allowing a finer control of the burst time. An alternative is to incorporate the active ingredient within the multi-layer films. Degradation of the film, triggered by changes in pH or other environmental stimuli, causes the gradual release of the drug. The release kinetics of protein during the degradation of multi-layer films has been studied by Wood et al.²⁰ and Macdonald et al.²¹ Hammond and co-workers have developed an interesting extension to the technique for inclusion of drugs in multi-layers.²² The active ingredient was first incorporated into nano-particles, consisting of co-polymer micelles. These nano-particles were then used as one of the components in the deposition of alternate layers, with the other component consisting of tannic acid.²² However, it must be noted that in this work the attractive interactions between different layers was due to hydrogen bonding, rather than electrostatic in origin. The use of LBL method also provides means for incorporating both hydrophobic and hydrophilic drugs, simultaneously, in the same dual delivery microcapsule.²³

The substrate upon which the multi-layer is grown is not always of a macroscopic size. In many applications this could be the surface of colloidal entities and therefore of mesoscopic dimensions. Notable examples of such systems involve coating of enzyme particles²⁴ by protective polymer films for pharmaceuticals applications, and that of emulsion droplets by polysaccharide layers in the field of food science.^{25, 26} Due to strong hydrophilicity of the majority of polysaccharides and a lack of sufficient charge at oil-water interfaces, these polyelectrolytes have little affinity for direct adsorption onto the surface of oil emulsion droplets. However, most food emulsions are traditionally prepared and stabilised using an initial layer of adsorbed protein. Proteins such as bovine milk α_{s1} -casein, β -casein and β -lactoglobulin, often used for this purpose, have isoelectric points in the pH range of 4-5. Thus, at pH values lower than pI, it becomes possible to deposit anionic polysaccharides onto the positively charged primary protein layer.^{25, 26} Emulsions stabilised by a secondary layer of polysaccharide have a number of distinct advantages compared to the traditional "protein only" stabilised emulsions. Reported results in the literature have demonstrated that these emulsions have a much better stability against freeze-thaw cycles and changes in pH and electrolyte concentrations, occurring during their processing.²⁷⁻³⁰ The polysaccharide film can also act as a barrier to digestive enzymes such as lipase, hindering their diffusion and access to the oil droplets. It has been suggested that this slows down the uptake of fat during digestion, hence providing a potential method for the design of healthier food products.³¹

Fabrication of multi-layers on the surface of colloidal particles or emulsions introduces a certain complication in the use of LBL technique, otherwise not present in coating of larger substrates. Colloidal systems are prone to aggregation if the nature of

interactions between particles or droplets changes from repulsive to an attractive one. Therefore, at every stage during the deposition, the colloidal stability of the system has to be assured. For protein stabilised emulsions part of this repulsion is provided by electrostatic interactions between positively charged protein layers.³² Adsorption of negatively charged polysaccharide, at the early stages of the formation of the secondary layer, can reduce the overall surface charge. This diminishes the electrostatic repulsion between the droplets. Furthermore, since at this initial stage of deposition, not enough polysaccharide is as yet adsorbed on the protein layers, the steric forces mediated by the secondary layer may not be strong enough to compensate for the reduction in electrostatic repulsion. This can lead to aggregation and breakup of emulsion, before enough polysaccharide accumulates at the surface of the droplets. The other possibility is that of bridging flocculation,³³ induced here by the simultaneous adsorption of negatively charged polysaccharide chains onto different positively charged protein layers, belonging to two closely spaced neighbouring droplets. One of the motivations for the current work is to examine the nature of colloidal interactions that arise from electrostatically formed multi-layers to ascertain the type of circumstances under which these instabilities can arise.

While the protein-polysaccharide multi-layers have been the subject of many experimental investigations, there are fewer theoretical or computer simulation studies involving these systems. This is to be contrasted to the case involving formation of protein-polysaccharide complexes away from the interfaces and within the bulk solutions.³⁴⁻³⁶ This, at least in parts, is due to the fact that in bulk one only needs to consider the interaction of a polysaccharide chain with one or a few protein molecules. This makes the study of such complexes quite amenable to simulation techniques such as Monte Carlo and molecular dynamics.^{34, 37-39} However, in most practical cases, the protein-polysaccharide multi-layers involve dense adsorbed layers of these polymers. A single polysaccharide chain not only interacts with many more protein molecules, when adsorbed at the interface, but also with many neighbouring polysaccharide chains having the same net charge as itself. Many of the more interesting and colloiddally relevant aspects of such films only manifest themselves in simulations involving a large numbers of adsorbed molecules. The MD simulations of multilayers formed by either short polyelectrolytes with various uniform charge densities or/and nanoparticles have been performed by Dobrynin and co-workers.⁴⁰⁻⁴³ In all these studies the authors also included strong short-ranged attraction between all the monomers. This is thought to be an important prerequisite for the occurrence of charge reversal and formation of multi-layers.⁴² The simulations provide valuable information on the dynamic of adsorption but remain rather time consuming. Fortunately, a different approach, based on the use of self consistent field (SCF) numerical calculation scheme, originally introduced by Fleer and Schutjens,^{44, 45} has been shown to work very well for such densely adsorbed protein interfacial layers,⁴⁶⁻⁴⁸ at least in so far as the equilibrium behaviour of these films is concerned. This is particularly the case for more coil like disordered proteins, such as α_{s1} -casein and β -casein, which have no tertiary and very little secondary structures.^{46, 47} In fact, the mean field nature of the method means

that it becomes increasingly more accurate, as the number of neighbouring molecules with which a chain interacts, becomes large.⁴⁹ In our previously reported work, we have extended this method to the study electrostatically formed protein-polysaccharide multi-layers^{49, 50} and those produced from adsorption of covalent complexes of protein and polysaccharides.⁵¹

On the basis of a simple argument, as the degree of the charging of the polyelectrolyte increases, so will its affinity for adsorption onto an oppositely charged surface. Therefore, a higher level of adsorption and a thicker deposited layer are expected to result. In the current work we shall show that, due to the electrostatic nature of the interaction, this may indeed not be the case. We also investigate the equilibrium state of the mixed protein + polysaccharide layers in order to identify circumstances where this film is a single mixed layer and those where it comprises of distinct individual multi-layers. It is known that polymers forming the multi-layers are capable of inter-diffusion.⁵² This causes the initial (and often the desired) structure of the film to evolve over a period of time towards a different equilibrium configuration. Such situation is particularly encountered where there is no drying of the substrate involved and the final product has to be stored in a wet environment (e.g. food emulsions). In a series of interesting experiments, Jourdain et al.⁵³ compared the dynamic interfacial tension behaviour of the mixed films of the protein, sodium caseinate, and the polysaccharide, dextran sulphate, adsorbed at n-tetradecane-water interfaces in two different ways. In the first of these, the adsorption took place in a single step from a mixed solution of these two biopolymers. In the second, an LBL type addition of the polysaccharide was made to an already prepared primary film of sodium caseinate. The variation of the interfacial tension was found to be significantly different for the two cases. This indicates markedly different rates of adsorption and contrasting initial structures for the two films. However, after around 20 minutes or so, the measured interfacial tensions were seen to approach the same value.⁵³ This is thought to be due to the evolution of the structure of the two films towards the same equilibrium configuration.

Finally, we also use our SCF calculations to investigate the influence of the heterogeneity of the charge distribution along the polyelectrolyte backbone, on the structure of the resulting multi-layers. We found that the competitive adsorption, between the more heavily charged segments of the chains and the lighter charged parts, turns out to be a significant contributor to the phenomenon of overcharging and reversal of the charge at the interface, during the adsorption of these type of polysaccharides. On the basis of experimental results alone, it is not entirely possible to infer whether the overcharging arises as a result of metastable film structures, or whether it is a phenomenon that also persists in the equilibrium state. We shall show that at least, for polyelectrolytes with a non-uniform degree of charge along the chain, it is the later that holds true.

The paper is organised as follows. In the next section we shall briefly highlight our SCF calculations as applied to protein + polysaccharide mixed/multi-layers. Next, we discuss our models for the protein and polysaccharides, respectively. We loosely base our “model protein” on the primary structure of milk protein α s1-

casein, retaining the same train of hydrophobic, polar and charged amino acid residues. We then present the results of our numerical calculations for the level of adsorption of polyelectrolytes onto a layer of this “model protein”, for various polysaccharides with the same chain length, but carrying different electrical charges. The data showing the influence of the charge heterogeneity on the equilibrium structure of the resulting interfacial layers is presented next. Finally, we discuss the problem of charge reversal arising from the adsorption of the polysaccharides.

2 Methodology and Model

2.1 Self-Consistent Field Approach

The properties of electrostatically driven protein-polysaccharide complexes at the interface are investigated using an implementation of self-consistent field (SCF) lattice theory, initially developed by Scheutjens and Fleer^{44, 45, 54-56} and later generalized to polyelectrolytes by Böhmer et al.⁵⁷ and Israels et al.^{58, 59} The method adapted to our protein-polysaccharide system was described in some detail previously⁵¹ and therefore only the main aspects of the theory are presented here. The studied system consists of protein, polysaccharide, ions, and solvent molecules distributed between two parallel plates in equilibrium with bulk solution. The space between the surfaces is divided into layers, $r = 1, 2, 3, \dots, D$ parallel to the plates, and each layer is further divided into lattice cells of equal volume. The simple cubic lattice with the lattice spacing of $a_0 = 0.3\text{nm}$ was used in the current approach. Each layer is fully occupied with protein residues, polysaccharide monomers, ions and solvent molecules. The Bragg-Williams approximation of random mixing is applied within each layer, and thus all lattice cells within a layer are assumed to be equivalent in terms of the concentration of various species. In our model we have five types of molecular components: the solvent ($i = 0$), the protein ($i = 1$), the polysaccharide ($i = 2$), cations ($i = 3$), and anions ($i = 4$). The protein chains are made form six different groups of residues while the polysaccharide consist of one or two monomeric species types denoted by α (see section 2.2). Therefore, depending on the polysaccharide structure, and taking ions into account, there are a total of either nine or ten species types α in the system.

In the SCF approach, each species α (i.e. solvent, different protein residues, polysaccharide monomers and ions) experience a potential of mean force, $u^\alpha(r)$ for that type. For any species α at distance r from the surface this potential of mean force can be expressed as a combination of three parts

$$u^\alpha(r) = u_{\text{hc}}(r) + u_{\text{int}}^\alpha(r) + u_{\text{el}}^\alpha(r) \quad (1)$$

In the above equation $u_{\text{hc}}(r)$ is a hard-core potential term, which has the same value for all types of species in layer r . It ensures that the space in each layer r is completely occupied and hence

$$\sum_{\alpha=0} \varphi^\alpha(r) = 1 \quad (2)$$

where $\varphi^\alpha(r)$ denotes the volume fraction of species α in layer r . The second term in eq. 1, $u_{\text{int}}^\alpha(r)$, represents a short-range

interaction and is expressed as

$$\mathbf{u}_{\text{int}}^{\alpha}(\mathbf{r}) = \sum_{\beta=0}^{N_{\text{type}}} \chi_{\alpha\beta} \left(\langle \phi^{\beta}(\mathbf{r}) \rangle - \Phi^{\beta} \right) + (\delta_{r,1} + \delta_{r,D}) \chi_{\alpha S} \quad (3)$$

Here $\chi_{\alpha\beta}$ is the Flory–Huggins interaction parameter between species of type α and β . Similarly, $\chi_{\alpha S}$ denotes the interaction parameter between species of type α and the surface (S), with $\delta_{r,1}$ and $\delta_{r,D}$ being the usual Kronecker delta functions and ϕ^{β} representing the bulk volume fraction of species β . Finally, the third term in eq. 1, $\mathbf{u}_{\text{el}}^{\alpha}(\mathbf{r})$, is a long-range electrostatic contribution and it is calculated as $\mathbf{u}_{\text{el}}^{\alpha}(\mathbf{r})$

$$\mathbf{u}_{\text{el}}^{\alpha}(\mathbf{r}) = q^{\alpha} \Psi_{\text{el}}(\mathbf{r}) \quad (4)$$

where q^{α} is the charge of the species α and $\Psi_{\text{el}}(\mathbf{r})$ the electrostatic potential in layer r . The electrostatic potential only varies with the distance away from the surface and it is set to zero in the bulk solution far away from the region between the two surfaces. The potential, $\Psi_{\text{el}}(\mathbf{r})$, is related to the variation of charge density in the space between the two plates through a suitably discretized version of the Poisson equation:

$$\epsilon_0 \epsilon_r \nabla^2 \Psi_{\text{el}}(\mathbf{r}) = -\rho(\mathbf{r}) \quad (5)$$

In eq. 5, $\epsilon_0 \epsilon_r$ is the permittivity of the medium, ∇^2 is the Laplacian operator, and $\rho(\mathbf{r})$ the space charge density in layer r . This volume charge density $\rho(\mathbf{r})$ can in turn be related to the plane charge density $\sigma(\mathbf{r})$, $\rho(\mathbf{r}) = \sigma(\mathbf{r})/a_0$, with a_0 being the thickness of each layer. The plane charge density is calculated according to

$$\sigma(\mathbf{r}) = \sum_{\alpha} q^{\alpha} \phi^{\alpha}(\mathbf{r}) \quad (6)$$

and is expressed in the units of e/a_0^2 in present calculations. Similarly, unless stated differently, the electrostatic potential, $\Psi_{\text{el}}(\mathbf{r})$, is given in units of $k_B T/e$.

The major quantities of interest in the SCF approach are the sets of potentials $u^{\alpha}(\mathbf{r})$ and volume fractions $\phi^{\alpha}(\mathbf{r})$. If potentials are known, one can obtain the volume fraction for any type of species α , and hence those for each molecular component i , in any layer r away from the surface.⁵¹ Obtaining values of $u^{\alpha}(\mathbf{r})$ and $\phi^{\alpha}(\mathbf{r})$ is the aim of SCF calculations and once these are determined it is a straight forward task to evaluate other system properties, such as: free energy of the system, electrostatic potential, adsorbed amount of different components, and the average location away from the surface for any monomer on the backbone of a polymeric chain. However, as it is seen from the equations above, the potentials $u^{\alpha}(\mathbf{r})$ is dependent on the volume fractions $\phi^{\alpha}(\mathbf{r})$, and vice versa. Therefore, in order to obtain the required values for these quantities, a set of non-linear equations is constructed and solved numerically by an iterative procedure. The convergence is achieved when the boundary conditions are satisfied and the volume fraction profiles are consistent with the mean-field potentials both in bulk and at the interface. We have checked the uniqueness of our solution by starting the iterations from many different initial starting conditions. For any given system, the iteration procedure was found to always converge to the same answer. It can be shown that the volume fraction

profiles obtained in this fashion are those that minimize the free energy of the system. The tolerance in the convergence was set in our calculations to be 10^{-7} .

2.2 Polysaccharide and protein models

The investigation here has been carried out using a look-alike model of α_{S1} -casein, based on the primary structure of this protein. This model has been described in detail elsewhere and is illustrated in Fig. 1 in our previous work.⁵¹ Therefore once again only a brief description is given here. The protein α_{S1} -casein is a disordered type protein due to presence of a large number of proline and lack of cysteine residues. It consists of 199 amino acids. In our model each amino acid is considered as a single residue. Therefore, together with N- and C-termini groups at two ends, our protein is a polymer chain consisting of 201 residues in total. In our model, different amino acids making up the protein chains are divided into six distinct groups according to their hydrophobicity and charge properties. These are hydrophobic, polar (non-charged), positively charged (two types, with different pK_a values), and negatively charged (again two types with different pK_a values). For most parts during our study we shall considered a bulk pH value of 3, where the protein possesses a strong net positive charge. At this same pH value the charge of the polysaccharide is negative, thus giving rise to the possibility of electrostatic complexation between protein and polysaccharide at the interface. The charge of each group type was calculated according to the assumed pK_a values⁵¹, so at pH = 3 the net protein charge was $Z_{\text{prot}} = +21.04e$.

The polysaccharides are modelled as linear polymers, comprising of blocks with different charge density, with a total polymer length of 500 monomers. An important aim of our study is to compare the adsorption behaviour of polysaccharides with a non-uniform distribution of charge on their backbones with those having a more uniform structure. Therefore, we have investigated and compared three types of polysaccharide models as follows:

- (I) Uniformly charged homopolymer A_{500} with the monomer charge varying from $Z_A = -0.01$ to $-2.0e$. This represents chains where charged groups are uniformly distributed along the backbone of the polysaccharide.
- (II) A polyelectrolyte with structure $A_{20}B_{480}$, but where in different systems the charge is increasingly concentrated on the shorter A_{20} block ($Z_A = -0.0496$ to $-1.24e$), while at the same time being reduced on the long B_{480} side ($Z_B = -0.0496$ down to 0). This is done in such a way so as to ensure that for all different polyelectrolytes considered, the total charge of the chains remains exactly at the same value of $Z_{\text{tot}} = -24.8e$. Apart from their charge, in every other respect “A” and “B” monomers are otherwise identical. The model represents the situation where the carboxyl or other charge groups are increasingly situated at one end of the polyelectrolyte (the “A” side), thus giving this end a higher average charge density compared to the rest of the molecule. In practice, of course, real polysaccharides will have a number of such more strongly charged regions and these may not necessarily lie at one end of the chains. Nevertheless, for the purpose of this preliminary study, our simple diblock model serves well as a starting point to contrast the difference in the structure of mixed layers formed by protein and homogeneous and non-uniformly charged polysaccharides.

(III) Diblock polyelectrolyte with the same structure as that in (II) above, but now with a fixed charge for the B monomers of $Z_B = -0.01e$. The charge for the A monomers is varied from a value of $Z_A = -0.25$ to $-3.0e$. Similarly, while keeping the charge on A monomers at a fixed value of $-1.0e$, Z_B is changed gradually from -0.005 to $-0.1e$. As well as having a non-uniform charge density, now chains in different systems also have a varying degree of overall charge, indicating higher or lower proportions of sulfated hydroxyl, carboxylated or other similar charge groups found on polysaccharides.

The models are illustrated schematically in Fig. 1 with exact charge distribution given in more detail in Table 1.

The Flory-Huggins interaction parameters between the different types of monomers are mostly taken from the previous work in the literature.^{47, 48, 51} The most important of these are as follows. The short-range interaction between the hydrophobic residues and all the other species types are set to be strongly non-favourable. Namely, $\chi = 2.0k_B T$ for the interactions between the protein hydrophobic residues (type 1) and polar ones (type 2) and $\chi = 2.5k_B T$ for those between the hydrophobic residues and all the other species types, including solvent molecules. The short range interactions between the ions and the solvent molecules are set to $\chi = -1.0k_B T$ indicating a favourable interaction due to the possibility of hydration of these ions by the solvent molecules. All the other remaining interactions in the solution are set to be athermal ($\chi = 0k_B T$). None of the species apart from the hydrophobic residues belonging to protein chains have any specific affinity for adsorption onto the surface of the two parallel plates (i.e. $\chi_S = 0k_B T$). For these hydrophobic residues we have a surface adsorption energy of $\chi_S = -2k_B T$ per monomer. This is typical of hydrophobic interactions between such residues and surfaces where both are hydrophobic. Note in particular that there are no favourable short range interactions between protein and polysaccharide in our calculations.

The bulk volume fractions of protein and polysaccharide was considered relatively low, that is, $\Phi_{CS} = \Phi_{PS} = 10^{-11}$ and kept constant throughout our calculations. The low values reflect the fact that most of these biopolymers will end up adsorbed onto the surface of the colloidal particles/emulsion droplets in typical colloidal systems of interest. This leaves the bulk concentration of protein and polysaccharide at a rather small value.⁴⁸ The volume fractions of salt used was $\Phi_S = 10^{-4}$. The calculations were carried out with a separation distance between the walls of $r = 400a_0$ unless stated otherwise. As such the two surfaces are sufficiently far apart so as not to interfere with each other, in so far as the adsorption of biopolymers on each wall is concerned.

3 Results

The structures of the protein-polysaccharide layers at the hydrophobic interface will be considered for each of the three polysaccharide model types, discussed in the previous section, separately. We begin by first considering the behaviour of a simple homopolymer polysaccharide model. Then we study the change in the structure of the mixed layer which arises when the uniformly charged homopolymer is replaced with a non-uniformly charged diblock model. This is done by gradual redistribution of charge along the chain, whilst keeping the total

polysaccharide charge constant. Finally, we explore the effects of the variation of charge in different blocks of the diblock polysaccharide model on the formation of the mixed biopolymer

Table 1 A summary of different charges (in units of e) for “A” and “B” monomers comprising our model polysaccharides, as used in our study.

Homopolymer A_{500}								
Z_A	-0.01,	-0.0496,	-0.07,	-0.1,	-0.2,	-0.3,	-0.5,	-0.7, -1.0, -1.2, -1.5, -2.0
Transition from A_{500} homopolymer to $A_{20}B_{480}$ diblock								
Z_A	-0.0496	-0.3	-0.52	-0.7	-0.85	-1.0	-1.12	-1.24
Z_B	-0.0496	-0.0392	-0.03	-0.0225	-0.01625	-0.01	-0.005	0
$A_{20}B_{480}$ diblock, Z_A varied, Z_B fixed								
Z_A	-0.25,	-0.35,	-0.5,	-0.7,	-1.0,	-1.1,	-1.5,	-2.0, -3.0 ($Z_B = -0.01$)
$A_{20}B_{480}$ diblock, Z_B varied, Z_A fixed								
Z_B	-0.005,	-0.01,	-0.015,	-0.02,	-0.03,	-0.05,	-0.1	($Z_A = -1.0$)

interfacial layer. The analysis of the interfacial complexes includes evaluation of volume fraction (monomer density) profiles for protein and polysaccharide, adsorption data, electrostatic potential distributions, and average distances from the surface for individual monomers along the polymer backbone.

3.1 Mixed layers formed by protein and uniformly charged polysaccharides

In our simplest model of polysaccharide all the monomers possess the same charge. A number of different cases where the charge density (charge per monomer) Z_A was varied from -0.01 to $-2.0e$ were studied. The adsorbed amount of protein at the interface and that of polysaccharide deposited onto the adsorbed protein layer were obtained using our SCF calculations. The adsorbed amount of each molecule i , θ_i , at the interface is calculated according to

$$\theta_i = \frac{1}{2} \int (\varphi_i(r) - \Phi_i) dr \quad (7)$$

where the integral is taken over the entire gap between the two (well separated) walls and $\varphi_i(r)$ and Φ_i represent the volume fractions of molecule i at a distance r from the first wall and that in the bulk solution, respectively. It must be stressed that the adsorbed amount refers to the excess amount of the biopolymer at the interfacial region and not just the molecules that are in direct contact with the walls. The results are plotted as a function of absolute polysaccharide monomer charge, $|Z_A|$, in Fig. 2. The adsorption of protein is seen to increase at first as the polysaccharide is made more negative. Such adsorption behaviour is not surprising. The adsorption of protein molecules to the interface is initially limited by their strong mutual electrostatic repulsion. The presence of stronger negatively charged polysaccharides reduces the net positive charge of the interfacial layer to a larger degree, thus allowing more protein to be adsorbed. However, the protein adsorption cannot increase indefinitely and eventually steric factors come into play which limits the casein adsorption. This is seen as the plateau in the corresponding graph in Fig. 2 for values of $|Z_A| > 1$.

The dependence of polysaccharide adsorption on its charge is rather different from protein. It is obvious that for zero or very

low $|Z_A|$ no polysaccharide chains are expected to adsorb onto the protein layer. To adsorb onto the oppositely charged protein film, the polysaccharide charge should be high enough to provide a sufficiently strong electrostatic attraction compensating for any loss in configurational entropy, suffered by the polymer upon its adsorption. With increase of charge the homopolymer adsorption initially increases. Naively one may expect this trend to continue, eventually reaching a plateau much in the same way as for protein, as the attraction between protein and polysaccharide is made stronger. Instead, it is seen that the amount of polysaccharide in the mixed film reaches a maximum at $|Z_A| = 0.1e$. Beyond this level of charge the amount of adsorbed polysaccharide falls off as the chains are made more negative. This is despite the fact that the amount of protein in the mixed film continues to increase. Further examination of our calculated results provides the reason for this unexpected behaviour, as will be explained later in this section. The results of Fig. 2 imply that there is an optimum level of charging for the polysaccharide chains at which the maximum adsorption takes place. For our model polysaccharide here this value occurs at a charge of $-0.1e$ per monomer. A similar result was also observed in our previous work,⁴⁹ where we consider grafted protein and a diblock polysaccharide model. In passing, it is worth mentioning too that with the homopolymer charge density of $Z_A = -0.01e$, the amounts of adsorbed monomers for both protein and polysaccharide are practically the same.

Volume fraction profiles for the protein and polysaccharide molecules within the mixed interfacial layer are presented in Fig. 3, respectively. A number of different systems, with varying degrees of electrostatic charge on polysaccharide chains, were studied. The profiles show the monomer density distribution for each biopolymer, plotted as a function of distance away from the wall surface. As such, these graphs provide information on the thickness of the adsorbed polymer layers and the degree of stretching of the chains.

Comparison of the graphs for protein in Fig. 3 (lines a-c) reveals that the protein layer becomes more extended with increasing charge of the polysaccharide. For $Z_A = -0.0496e$, the protein layer has a thickness of $r \approx 10a_0$, with overwhelming majority of the residues situated within a distance of less than $5a_0$ from the surface. For $Z_A = -1.0e$ the film has now extended to $r \approx 15a_0$, and a far greater proportion of protein residues are found at distances beyond $5a_0$. This is in line with the result of Fig. 2, where a larger amount of adsorbed protein, resulting in a thicker film, was found for systems involving polysaccharides with higher negative charges. Also the graphs for polysaccharide, lines d-f, indicate that, the more highly charged polysaccharides are more intimately incorporated within the protein layer, which may also contribute to a more extended protein film. For example, with a charge of $Z_A = -0.0496e$ per monomer, polysaccharide extends to distances of around $r \approx 18a_0$. Similarly, for the same system, the peak in polysaccharide volume fraction occurs at $r \sim 4-5a_0$. At just over twice this charge, i.e. $Z_A = -0.1$, the corresponding values are $r \approx 15a_0$ and $r \sim 3-4a_0$. With further increase in the polysaccharide charge, the location of the maximum continues to shift closer to the surface and the overall thickness of the polysaccharide layer steadily decreases.

It is also interesting to note that the maximum value attained

by the volume fraction of polysaccharide is not a monotonic function of its charge. Initially the value of the peak increases from $\varphi_{PS} \approx 0.09$ to $\varphi_{PS}(r) \approx 0.15$, when charge per monomer is changed from $Z_A = -0.0496e$ to $-0.1e$. But then it drops down to 0.14, 0.11 and finally 0.07 as the polysaccharide charge is increased further to -0.3 , -0.5 and $-1.0e$ (data are only shown for $Z_A = -1.0e$ case). Once again, this finding supports the existence of an optimal level of polysaccharide charge for its highest level of adsorption on or into the protein film. Since the more negatively charged polyelectrolytes are expected to have a stronger affinity for the positively charged protein layer, this result may at first seem somewhat surprising and therefore merits some further explanation. As mentioned previously, the adsorption of polymers onto an interface involves loss of some configurational entropy. Therefore, a certain minimum strength of favorable interaction between the polysaccharide molecules and protein layer is required to compensate for this entropy loss before the adsorption of polysaccharide can take place.⁵⁴ Above this threshold, as the polysaccharide is made more negative, its affinity for the oppositely charged protein layer increases. This at first causes a rise in the amount of polysaccharide in the interfacial layer, as seen in Fig. 2. However, deposition of negatively charged polyelectrolyte, reduces, neutralizes and in some cases even reverses the charge of the protein film. This hinders and eventually limits further adsorption of the polysaccharide chains. For highly charged polysaccharides, this effect is established with a far smaller number of deposited molecules. This then explains the drop in the amount of adsorbed polysaccharide for more highly charged chains and the existence of an optimal value of charge for the maximum deposition (see Fig. 2). In this respect, there is a fundamental difference between deposition of polyelectrolyte onto a protein film, driven by non-specific long range electrostatic forces, and that involving more specific shorter range interactions such as, calcium bridging, hydrogen bonding or hydrophobic attraction. For the second case, the amount of adsorbed polymer is not expected to drop with increased strength of interactions.

Comparison of the profiles for both biopolymers at the same charge (lines a and d, b and e, c and f in Fig. 3) reveals another interesting feature of the interfacial layer. For systems involving lightly charged polysaccharide ($Z_A = -0.0496e$), most of the protein at the interface is confined to a short distance ($< 5a_0$) adjacent to the wall. On the other hand polysaccharide chains extend much further to distances of $r \approx 18a_0$. Thus, the biopolymer in the inner part of the interfacial film is predominately protein, whereas the outer part has very little protein and essentially consists of polysaccharide. As such, it is quite appropriate to think of the interfacial film as a multilayer, consisting of a primary protein and secondary polysaccharide layers. This is to be contrasted with the case of more highly charged polysaccharide. As we described above, the protein layer expands and polysaccharide layer contracts with increasing charge of the latter. For $Z_A = -1.0e$, no distinct parts of the interfacial layer can be identified which are purely dominated by one or the other of the two biopolymers. The film now has a much more uniform and mixed structure. A similar result was also observed in our previous work,⁵⁰ where complexes of grafted casein with long ($N = 1500$), strongly charged ($Z_A = -2.0e$),

polyelectrolytes were considered. We emphasize that our findings refer solely to equilibrium structures, towards which we believe the interfacial layers will slowly evolve. But these do not preclude the possibility of emergence of other, perhaps long lived “metastable” states, arising due to the dynamics of a particular processing condition. Nevertheless, MD simulations of LBL deposition involving relatively short polyelectrolytes have further confirmed a high level of intermixing between the two sets of adsorbing chains.⁴²

Further information regarding the spatial distribution of biopolymer molecules within the interfacial layer can be obtained by calculating the average distance from the surface for individual monomers of protein and polysaccharide. Results of such an exercise are presented in Fig. 4. Fig. 4a shows average distance from the surface for each protein residue, with three curves representing systems with different polysaccharide charges, $Z_A = -0.0496$, -0.1 , and $-1.0e$. With a low charge, $Z_A = -0.0496e$, the adsorbed α_{S1} -casein at the surface behaves like a “diblock”, with most of its monomers located near the surface, forming a “train”, and only a few monomers at the N-end protruding into the solution for distances up to $r = 7a_0$. Note that in absence of polysaccharide, α_{S1} -casein on its own adopts a configuration more akin to those expected for a tri-block polymer.^{46, 51} With increase in the polysaccharide charge, the middle part of the molecule also starts to desorb from the surface and stretches further away, forming a “loop”. As polysaccharide becomes more negative, the larger and more extended the loop section becomes. At the same time, the tail end at the N-terminus becomes less stretched. Altogether, we can see that with increase of Z_A the overall distribution of protein monomers becomes more extended and protrudes further away from the wall. The changes in the typical configuration of protein with increase in the polysaccharide charge correlates well with graphs for the volume fraction profile, seen in Fig. 3.

The average distance from the surface for each polysaccharide monomer, labeled 1 to 500, is displayed in Fig. 4b. Since for a homopolymer all the monomers are identical, the distributions are symmetric with respect to the centre of the chain, with all monomers located approximately at the same average distance from the wall. The small difference in the average position between the monomers in the central part of the chain and those at the end, is due to well known entropic reasons.⁵⁴ Tail monomers have a larger number of conformations available to them in the bulk than those for the connected central ones. Consequently, entropic penalty upon adsorption is greater for these tail ends, keeping them somewhat further away from the surface. Similar effect of dangling tails was observed in Monte Carlo simulations of complexation between a charged sphere and an oppositely charged polyelectrolyte.^{34, 35} Our distributions of the polysaccharide monomers show that with increase of negative charge the average location of the whole chain shifts closer to the surface. This effect is once again in line with the volume fraction profiles (Fig. 3), where we observed a shift in the location of maximum polysaccharide density towards the surface, for higher $|Z_A|$.

3.2 Interfacial layers involving non-uniformly charged polysaccharides

In many naturally occurring and synthetically modified

polysaccharides the distribution of charge groups is far from uniform along the backbone of the molecules. In this section, we shall study the changes in the structure of protein + polysaccharide interfacial films that arise as a result of this heterogeneity of the charge distribution. We adopt the simplest possible model that can capture the behavior of a non-uniformly charged polyelectrolyte, namely a diblock polymer. We start with a system containing the homopolyelectrolyte of the previous section with a monomer charge of $Z_A = -0.0496e$, resulting in a total charge of $Z_{tot} = -24.8e$. Next a series of systems are considered in which the homopolymer is replaced with the diblock model for the polysaccharide, composed of a short “A” block (20 monomers) and a long “B” block (480 monomers), denoted by $A_{20}B_{480}$. The charge of A-monomers is gradually increased from one system to the next, from $Z_A = -0.0496e$ to $Z_A = -1.24e$. At the same time the charge of B-monomers is reduced from $Z_B = -0.0496e$ to $Z_B = 0$, such as to keep the total charge of diblock chains at the same value as the reference homopolymer, $Z_{tot} = -24.8e$. Such a step-by-step re-arrangement of charge allows the effects of transition from a homogeneously charged homopolymer to a diblock with a non-uniform charge distribution to be systematically studied. In the “extreme” case, the whole polysaccharide charge is located within the short A section leaving the long B-block electrically neutral.

Fig. 5 shows the adsorbed amount of protein and polysaccharide, as given by eq. 7, plotted as a function of absolute charge of A-block monomers, $|Z_A|$. The charge of B-block monomers is adjusted accordingly, as mentioned above. The adsorbed amount for both biopolymers increases with a higher level of charge heterogeneity of the diblock polysaccharide. Thus, despite the fact that in all of these systems the polysaccharides have exactly the same charge, the diblock polysaccharides with a short highly charged block and a long weakly charged one, seem to enhance the deposition of protein, as well as adsorbing more extensively themselves onto the protein layer.

Volume fraction profiles of polysaccharide, shown in Fig. 6, illustrate how the thickness of polysaccharide layer alters with increasing level of charge heterogeneity. Diblock polysaccharide with the short highly charged section and long weakly charged block, gives a much thicker and more distinct secondary layer compare to uniformly charged homopolymer of the same overall charge. The interfacial layer for the diblock chain, where the entire charge is located on the first 20 monomers (i.e. $Z_A = -1.24e$ and $Z_B = 0$) stretches for distances in excess of $r \approx 70a_0$ away from the surface. This is nearly four times as far as that observed for the homopolymer case ($Z_A = -0.0496e$), where $r \approx 18a_0$. With gradual accumulation of charge at one end, and with increasing extension of the polysaccharide layer, the maximum in volume fraction attains a smaller value and its location shifts slightly further away from the surface. Increasing the charge of the A-block even more, causes the polysaccharide profile to become bimodal. This is quite typical of diblock co-polymers consisting of monomers with very different adsorption affinities.⁵⁴ The narrow part of the profile, with a maximum near the surface, arises predominately from the highly charged A monomers. This is followed by a second, more spread out distribution with its maximum some distance away from the

surface. The latter consists mainly of the long weakly charged (or uncharged, as the case might be) B-blocks. In contrast, the thickness of the protein layer does not change greatly with variation of polysaccharide charge distribution. This is despite the fact that the amount of adsorbed protein increases with the degree of polysaccharide charge heterogeneity.

The average distances away from the surface for individual monomers of the diblock chains are displayed in Fig. 7. The distributions differ significantly from those obtained for the homopolymer case (Fig. 4b) and follow the same trend as the already discussed data in Fig. 6. It is seen that the monomers of the short highly charged A-blocks are all located very near the surface ($r \approx 2-3a_0$), while the B-blocks stretch well away into the solution. The weaker the charge of the B-monomers, the further away from the surface the long B-blocks extends. For the limiting case, $Z_B = 0$, the average distance away from the surface for the end monomers is $r \approx 40a_0$. This is considerably further than that seen for the uniformly charged chains, with $r \approx 7-8a_0$. This result has important implications for the nature and range of colloidal interactions between particles and emulsion droplets, covered by such mixed / multi-layers. We shall defer a discussion of this to a future publication.

Results of Figs. 5, 6 and 7 provide clear evidence that the net charge of the polyelectrolyte is not the only factor controlling the amount of adsorption and the structure of the interfacial layer. The manner in which the charge is distributed along the backbone plays an equally important role in determining the adsorption behaviour. For the case of our simple diblock model, the picture that emerges is as follows. The more highly charged A and lightly charged B blocks compete with each other for adsorption (or onto) the protein layer. When the charge density of the two is similar, they both adsorb equally and the configuration adopted by the polysaccharide is relatively flat as it lies within the surface layer. Making A monomers more negative and B ones less charged, causes more A-blocks to adsorb, replacing longer B-blocks which now dangling away from the surface. The configuration of polysaccharide approaches the one seen for "brushes".⁵⁴ The chains are now more extended as was indicated by the results of Figs 6 and 7. Displacement of long B-blocks, and their replacement by many shorter A sections, allows for the involvement of a larger number of deposited chains. Consequently, the amount of adsorbed polyelectrolyte increases as their charge distribution becomes more non-uniform, as is illustrated in Fig. 5.

Before we end this section we also mention that for the case of diblock model, with light, but non-zero charged B-blocks, the charge of the protein layer becomes overcompensated by the adsorption of polysaccharide. Thus, the interfacial film reverses its charge from positive to negative. This effect is clearly seen in many experiments and will be discussed in more detail in section 3.4.

3.3 Changes in the interfacial layer resulting from variation of the block charge densities.

In this section, we examine the influence of the charge densities of each of the blocks of $A_{20}B_{480}$ polyelectrolyte model of previous section, on the thickness and structure of the mixed interfacial biopolymer layer. First, the average charge of the B monomers is kept fixed at a relatively low value of $Z_B = -0.01e$, while different

chains with Z_A values varying from -0.25 to $-3.0e$ are considered. Next, we maintain Z_A at quite a high charge of $-1.0e$, and allow Z_B to change from $-0.005e$ to $-0.1e$. Unlike the cases discussed in the section 3.2, now it is the charge of one or the other block that are kept constant, rather than that of the whole molecule.

In Fig. 8a we display the calculated change in the amount of adsorbed protein and polysaccharide due to variation in the charge of the A monomers. As $|Z_A|$ increases, the total charge of the chains varies from a rather low value of $Z_{tot} = -9.8e$ at $Z_A = -0.25e$ to a fairly high one of $Z_{tot} = -64.8e$ when $Z_A = -3.0e$. Initially, the adsorbed amount of polysaccharide is low when $|Z_A|$ is small, but it increases as $|Z_A|$ is made larger. The adsorbed amount attains a maximum value for $|Z_A| \approx 1.0e$ and decreases thereafter as the A-blocks are made even more negative. This behaviour is the same as the one predicted for the homopolymer case in section 3.1. It reflects the more dominant role that the highly charged A-block plays in the adsorption of polysaccharide, when compared to the weakly charged B section. It is mostly the A monomers that are incorporated into the primary protein layer, with B-blocks dangling further into the solution. Thus, it is the affinity, and therefore the charge of these A monomers that determines the adsorption amount of polysaccharide. As $|Z_A|$ increases from a low value, the strength of attractive interactions between the A-blocks and the positively charged protein film becomes bigger, resulting in adsorption of more polysaccharide. But just as was the case with the uniformly charged chains of section 3.1, for highly charged A monomers, it takes the adsorption of a relatively small number of A-blocks to neutralise and reverse the charge of the biopolymer layer. The interplay between these two competing effects leads to an optimal value of Z_A , at which the maximum adsorption occurs. The same behaviour is not seen in the corresponding graph in Fig. 8b, where now it is the charge of the B monomers which is altered. Since $|Z_B| \ll |Z_A| = 1.0e$ throughout the range studied, we believe that making B monomers more negative does not significantly alter the affinity of the polysaccharide chains for the protein layer. All that such an increase in $|Z_B|$ leads to is the establishment of a net negative surface film with fewer chains involved, reflected as a monotonic drop in the adsorption level of polysaccharide with $|Z_B|$ in Fig. 8b. The increase of polysaccharide charge, whether achieved through higher $|Z_A|$ or $|Z_B|$, in both cases results in an increase in the protein adsorption, much in the same way as was discussed for the homopolymer chains (Fig. 2).

Fig. 9 illustrate the volume fraction profiles for a number of different polysaccharides, with various values of Z_A and Z_B , in the interfacial region close to the wall. In Fig. 9a, Z_A changes and Z_B is constant. When the charge on the A-block is low, $Z_A = -0.25e$, the volume fraction distribution has a single small maximum with $\phi_{PS}(r) \approx 0.012$ occurring at a distance $r \approx 8-9a_0$ from the wall. At distances further than this, the volume fraction falls but with values significantly different to bulk value persisting up to a distance of $r = 30a_0$. With a higher charge for A monomers, both the maximum value of $\phi_{PS}(r)$ and the layer thickness increase, reaching their largest values at $Z_A = -1.0e$. The curves in these cases have a bimodal behaviour, typical of block co-polymers as was mentioned before. The polysaccharide layer now extends up

to $r \approx 75a_0$. Making the A-blocks even more negative, leads to a decrease in size of both maxima in the volume fraction and a larger separation between where they occur. The overall thickness of the polysaccharide layer also becomes slightly smaller. The information from the volume fraction profiles regarding the interfacial layer thickness, suggests the same trend as was seen above. This can be summarised as follows. (I) a small number of adsorbed polysaccharide chains, most likely in coil like configurations, laying on or within the protein layer at low values of $|Z_A|$. (II) A more extended profile is observed as Z_A is made more negative and a far larger number of chains adsorb. These have their weaker charged B-blocks stretching well away from the surface in a more “brush” like configuration. Finally, (III) a drop in number of adsorbed chains occurs, accompanied by a decrease in the interfacial layer thickness. This happens when A-blocks become highly charged ($Z_A = -3.0e$) and a lesser number of chains are needed to balance the positive charge of the primary protein layer. In Fig. 9b, the volume fraction profiles for several cases where Z_B varies and Z_A is maintained at a constant value are displayed. These graphs are quite similar to those in Fig. 6. At low values of $|Z_B|$, a broad and distinct polysaccharide layer is observed at outer parts of the interracial film where very little or no protein resides. This polysaccharide layer becomes more condensed near the surface with increasing negative charge of the B-block. However, taking these profile distributions together with ones for the same diblock model where Z_A is varied (Fig. 9a), we notice that formation of such well extended and distinct polysaccharide layers requires a sufficiently high charge on A-blocks, as well as a low charge for B-blocks of the chains.

More support for the above conclusion can be obtained by examining the average location of individual monomers of the polysaccharide. In Figs. 10a and 10b, we have plotted the calculated average distance away from the surface, for each monomer, against its sequence number along the polysaccharide backbone. The numbering of monomers starts from the chain end where the A-block resides. A few different cases, with varying values of Z_A or Z_B have been included in Figs. 10a and 10b, respectively. In both graphs all the 20 monomers of the higher charged A-block are located close to the surface, at typical distances of $r \approx 2-3a_0$. The long block comprising of B-monomers extends far further, with the location of the end B monomer on the chain varying anywhere from $r \approx 12-13a_0$ up to $r \approx 37-38a_0$, depending on values of Z_A and Z_B . The degree to which the B-block protrudes into the solution is strongly depends on the combination of both charges, Z_A and Z_B . When both Z_A and Z_B are low (Fig. 10a, line a), the adsorbed chains are in coil like conformations and do not stretch far away from the wall. When both Z_A and Z_B are relatively high (Fig. 10b, line d), both blocks of the chains are strongly attracted by the net positively charged proteins at the interface. As such, the polysaccharide molecules tend to lie flat on the surface, in a rather similar manner as was observed for the homogeneous highly charged chains in section 3.1. We have not considered the situation, where Z_A is low but Z_B is high, as it is obvious that in this case the diblock will once again behave as a highly charged homopolymer with the whole molecule residing close to the surface. In this case the lightly charged A-block is too short to be able to protrude far from the wall. It also suffices to say that in all these cases the structure of

the interfacial biopolymer film is closer to a mixed one, rather than a multi-layer with its clear and separate protein and polysaccharide sub-layers. The greatest extension of the adsorbed polysaccharide chains, to distances as far as $r \approx 37-38a_0$, is observed when Z_A is high and Z_B is low (Fig. 10a, lines c, d and Fig. 10b line a). In this case the interfacial film develops a multi-layer type structure, with regions very close to the wall essentially dominated by the protein and the outer parts of the film consisting entirely of polysaccharide.

Although all the results presented in sections 3.2 and 3.3 were obtained for chains with the short highly charged A section at one end of the molecule ($A_{20}B_{480}$), we also considered other systems where the A-block was placed elsewhere along the backbone. In particular, we repeated many of the calculations for the case where the highly charged section was in the middle of the polymer. Qualitatively, the results followed the same trends as those reported here and led to precisely the same conclusions. In practice, polysaccharide chains will have a host of different ways in which the charge groups will be distributed along the length of the molecule. These results will be presented in more detail in a follow up paper. But nevertheless, the results presented here serve to show that multi-layer structures involving protein + polysaccharide, at equilibrium, are best achieved by using polysaccharide molecules where large parts of the polymer are lightly charged, with smaller sections containing a high density of charged groups.

3.4 Electrostatic potential

In the sections above, we examined how the adsorbed amount of protein and polysaccharide and the structure of the interfacial biopolymer film depend on the magnitude and the nature of charge distribution on the polysaccharide chains. An important component of the mean potential felt by charged species, at any given location away from surface, is the electrostatic potential at that point (see eq. 1). As such, the electrostatic potential, $\Psi_e(r)$, strongly influences the configuration and spatial distribution of the charged molecules, but in turn itself is specified by such distribution of charged residues, through Poisson equation (eq. 5). Since the determination of electric potential is an integral part of SCF scheme and available following calculations of the previous sections, it is useful to study it here and see if further information can be gained from such data.

The graphs for the variation of electrostatic potential with distance away from surface, for all of the polysaccharide models described above, have been presented in Fig. 11. Fig. 11a shows the results for the homopolymer case, while the data for systems containing the non-uniformly charged polysaccharide molecules are displayed in Figs. 11b to 11d. In all cases the background electrolyte volume fraction is 10^{-4} and $\text{pH} = 3$, where our $\alpha\text{S1-casin}$ like protein has a net positive charge. The electrostatic potential is measured with reference to a point far from the surface, inside the bulk solution. Of course, bulk solution itself is electroneutral. For all systems, at distances well outside the adsorbed biopolymer film, the electric potential drops in an approximately exponential manner, in line with Debye-Huckel theory for electrified interfaces.^{33, 60} The curves for homopolymer systems (Fig. 11a) are relatively easy to understand. In absence of polysaccharide, we have a thin adsorbed protein layer with a net

positive charge. Beyond this film, potential remains positive but decreases within the usual diffuse double layer formed by the ions of the background electrolyte. When weak, uniformly charged polysaccharide molecules are introduced, we saw in section 3.1 that these formed a mixed layer with the protein. Thus, incorporation of the negatively charged polysaccharide chains, present in rather flat conformations on the surface, simply serves to reduce the net positive charge of the interface. As a result the surface potential, defined by the value of $\Psi_{el}(r)$ at the outer edge of the mixed biopolymer film, also decreases, causing a drop in the electric potential everywhere else within the diffuse double layer. Apart from this effect then, the overall picture is not significantly altered by the incorporation of such polysaccharide molecules. This can be seen in the graphs of Fig. 11a, for systems involving polysaccharides with charge densities of $-0.0496e$, $-0.1e$ and $-0.3e$ per monomer. The higher the charge of the polysaccharide, the lower the potential is at any given distance away from the surface. Of course, the contribution of negative charge by polysaccharide to the adsorbed biopolymer layer also depends on the number of adsorbed chains, and not just their charge. We recall from the results of Fig. 2, that the maximum adsorption for our model polysaccharide occurs at a charge of $-0.1e$ per monomer. Thus, it is quite conceivable that increasing the monomer charge from $-0.1e$ to $-0.3e$ can actually lead to a decrease in the total negative charge, contributed by the polysaccharide to the interfacial film. However, this turns out not to be the case. The number of adsorbed chains only drops by a factor of ~ 1.5 , which is not enough to offset the tripling of the negative charge on each chain. This trend continues with further increase of the charge density of polysaccharide molecules. The electric potential at the outer edge of the biopolymer film eventually becomes zero, and then even very slightly negative, as more highly charged chains are considered. This can be seen in the two remaining graphs of Fig. 11a, representing systems with polysaccharide charges of $-0.5e$ and $-1.0e$ per monomer. The potential in the double layer region beyond the polymer film is now clearly observed to be negative for these two higher charged cases. However, we must stress that the degree of overcharging seen here is very small and the biopolymer films are almost neutral in these two latter systems. In particular, the minima of the electric potential, as seen in the corresponding graphs of Fig. 11a, are only -0.35 to $-0.4mV$. This is about an order of magnitude smaller than experimental data obtained using ζ -potentials measurements.^{29, 30, 53, 61} This situation is altered dramatically for non-uniformly charged polysaccharides, as evident from the data presented in Figs. 11b to 11d. For these systems, our calculations predict negative surface potentials much closer to experimental findings. We shall discuss the electric potential variation in these non-homogeneously charged polysaccharide systems next.

In Fig. 11b we present our calculated results for the electrostatic potential for cases involving $A_{20}B_{480}$ diblock polysaccharide models of section 3.2. Several different graphs are shown. For all of these, the total charge on each polysaccharide chain was kept fixed at $Z_{tot} = -24.8e$, but it was divided differently between the long B and the shorter A-blocks in each case. This provided the required variation in the distribution of charge along the polysaccharide backbone. The result for a

uniformly charged case, with the same total charge as others, has also been included. This is represented by the bold line in Fig. 11b. A comparison of different graphs reveals the subtle interplay between the direct effect of the charge of B monomers on $\Psi_{el}(r)$ on one hand, and the indirect way in which it alters the electric potential due to its influence on the structure of the biopolymer film. Initially as the charge distribution on polysaccharide molecules becomes increasingly more non-uniform, we obtain a minimum in $\Psi_{el}(r)$ graphs which attains lower values with increase of Z_A and decrease of Z_B . The minimum is $-6.3mV$ for $Z_A/Z_B = -0.52/-0.03$ and reaching values as low as $-24.9mV$ for $Z_A/Z_B = -1.0/-0.01$. However, this trend does not continue. For chains with even more highly charged A-blocks, and subsequently weaker charged B-blocks, the negative values for the electric potential become less pronounced one again. The lowest value of $\Psi_{el}(r)$ is only $-13.7mV$ for $Z_A/Z_B = -1.12/-0.005$. Finally, when the B monomers are made to be uncharged, i.e. $Z_A/Z_B = -1.24/0$, the potential is found to be positive everywhere.

The interesting difference in the variation of electric potential for different systems considered above can be understood as follows. When the charge of the B-blocks becomes too weak the chains were seen to protrude far away from the surface. We had a multi-layered type film, with a relatively thick outer layer consisting of weakly charged sections of polysaccharide. In fact, the largest extension was observed for the cases where all of the charge was concentrated in the A-block and B monomers were not charged at all (Fig. 7). The hydrophilic uncharged B-blocks have no affinity for the positive protein layer and therefore tend to avoid the surface in as much as possible. This is in order for them to minimize the loss of configurational entropy. Nevertheless, despite its larger extension, this secondary sub-layer does not lead to a distinct region of negative charge in the biopolymer film, since the B monomers are neutral. With position of B monomers not relevant and the short negatively charged A-blocks residing well inside the interfacial layer (see Figs. 6 and 7), overlapping the primary protein layer, we arrive at situation which resembles the homopolymer case. That is of course not in terms of the structure of the biopolymer layer, but rather in so far as distribution of charge at the interface is concerned. Thus, the observed similarity between the curves $Z_A/Z_B = -1.24/0$ and the corresponding one for uniformly charged polysaccharide, as seen in Fig. 11b. If we now consider the other limiting possibility, where the values of Z_A and Z_B are not all that different to each other, we are once again back to a situation that is close to a system with uniformly charged chains. Here we saw that a mixed protein + polysaccharide interfacial film resulted with no distinct region that is dominated by either biopolymer. Therefore, it is only in intermediate range of values of Z_B , where the charge of B monomers is still considerably smaller than Z_A for B-blocks not to compete with A, but yet not so small as for it to have a negligible contribution, that a reversal of surface potential can be expected. For such values of Z_B , the outer part of the interfacial film consists of a reasonably thick layer, which now also has a sufficient amount of charge to be seen as a negative surface from the bulk side (as for example will be the case in ζ -potential measurements). We also notice that for a range of values of $Z_A/Z_B = -0.7/-0.0225$, $-1.0/-0.01$ and $-1.12/-0.005$, the calculated electric potentials have minimum values that are of the

order of tens of mV, in good agreement with the magnitude of the reversed surface potential found experimentally for a number of protein + polysaccharide systems.^{29, 30, 53, 61}

The results in Figs. 11c and 11d are for model systems of section 3.3. The electrostatic potential, $\Psi_{el}(r)$, for the cases of non-uniformly charged polysaccharide $A_{20}B_{480}$ with different values of Z_A at constant $Z_B = -0.01e$, and changing values of Z_B where $Z_A = -1.0e$, are presented in Figs. 11c and 11d, respectively. The results reinforce what was observed in Fig. 11b. Once again when both Z_A and Z_B are low, $\Psi_{el}(r)$ is always positive. The low amount of adsorption, coupled with the fact that chains do not extend far for polymers with simultaneously low values of both Z_A and Z_B , is responsible for the lack of reversal of the sign of surface potential in such cases. When the charge of the A-blocks increases, but Z_B is kept low, the surface potential becomes negative. We saw in previous section, that for a fixed value of Z_B , the amount of adsorbed polysaccharide at the interface showed a maximum with variation in Z_A . For our chosen value of $Z_B = -0.01e$, this occurred at $Z_A = -1.0e$ (see Fig. 9b). Thus, not surprisingly, the largest degree of reversal of surface potential in Fig. 11c is also observed for the same system. With further increase in the charge of A monomers to $-3.0e$, the magnitude of the surface potential slightly decreases, as the amount of adsorbed polysaccharide chains drops. The minimum value of $\Psi_{el}(r)$ is now -23.1mV . Finally, let us consider the diblock polyelectrolyte model with Z_A set to the optimum charge of $-1.0e$, while we vary the charge of B-block. The results for such an exercise are shown in Fig. 11d. Here the electrostatic potential behaves in a similar manner to the case of the fixed total polysaccharide charge, shown in Fig. 11b. The reversal of the surface potential from positive to negative becomes more pronounced at first as Z_B is gradually made more negative. The interfacial potential, $\Psi_{el}(r)$, attains its most negative values at -24.9 mV when $Z_B = -0.01$, and -25.3 mV at $-0.03e$. Beyond this point, the additional increase in charge of B monomers is more than offset by shrinking of the polysaccharide layer (see Figs. 9b and 10b), and gradual transition of the multi-layer to a mixed layer. This is seen for the graphs of Fig. 11d, where $Z_B \geq -0.05e$.

In summary, for the simple model used here, the maximum reversal of surface potential was observed when the value of Z_A was close to its optimal value, leading to the largest level of adsorption of polysaccharide molecules. However, even in this case, the reversal would not occur unless a certain condition is met. The value of $|Z_B|$ has to be moderately low (compared to $|Z_A|$) so as to allow the formation of a multi-layer type interfacial structure, but sufficient for the secondary polysaccharide layer to make a reasonable contribution to charge of the interfacial film. While our model is of course too simple to provide a complete representation of many polysaccharides, it nevertheless serves to show that negative surface potentials, of the right order of magnitude as those in experiments, can easily arise from such non-uniform distributions of charge groups on the polymer. Although undoubtedly there are other factors that can also explain the reversal of charge, we believe that the heterogeneity of the charge distribution is at least an important contributory factor, that so far been overlooked, in understanding of this phenomenon. This is particularly the case where the interfacial

film is allowed to age and therefore has sufficient time to reach its equilibrium configurations.

4 Discussions and Conclusions

Inspired by the experimental results of Jourdain et al.,⁵³ we have applied the Self Consistent Field (SCF) approach to simple models of protein + polysaccharide, to gain some theoretical insight into the equilibrium structure of the mixed interfacial films. In particular we ask whether stable multi-layer structures can exist as true equilibrium configurations, and if so under what circumstances. Despite the simplicity of our models, we believe that they capture enough of the essential features of the two biopolymers, in so far as the formation of electrostatically driven layers is considered, for us to answer these questions. For the protein we use a model based on the primary structure of the bovine protein α_{s1} -casein. This disorder coil like protein, with little secondary and no tertiary structure, lends itself well to treatment by SCF method,^{48, 49, 51, 62} something that is not true for globular proteins. Polysaccharides are modelled as linear polyelectrolyte chains that are either uniformly charged, or have a section that is more heavily charged than the rest of the molecule. Again in using the latter, our aim has been to investigate the importance of the non-uniform distribution of charged groups along the polysaccharide backbone, on the structure of the resulting mixed layer.

For uniformly charged polysaccharide we find that the adsorption is affected by two competing considerations. On one hand, the affinity of the polysaccharide chains for the positive protein layer gets stronger as they become more negatively charged. This has the effect of increasing the amount of adsorbed polysaccharide at the interface. But on the other hand, if the chains are made too highly charged, deposition of a small number of chains suffices to neutralise, and even reverses, the electrostatic potential of the protein layer on the surface. This has the effect of hindering further adsorption of polysaccharide. The lower level of adsorption of more highly charged polyelectrolytes has also been found in the molecular dynamic simulations of Patel et al.⁴¹ Thus, it is evident that the maximum degree of adsorption occurs at some optimal level of charge for chains, occurring as a compromise between the above two opposing effects. Our calculated results clearly demonstrate existence of such a peak. We also find that the equilibrium structure of the interfacial layer is closer to a mixed film, rather than a multi-layer. This is more evident in systems where polysaccharide is strongly charged, beyond the optimum value for its adsorption. Increasing the negative charge on the chains reduces the number of adsorbed polysaccharide molecules. It also causes them to protrude less into the solution as they adopt flatter conformations at the interface. At the same time, we observe that the middle, more hydrophilic section of α_{s1} -casein, forms a more extended loop away from the surface. Protein and polysaccharide are seen to be strongly overlapping. It is rather difficult to distinguish a clear "secondary" polysaccharide layer, distinct from the primary protein film, in such cases. When the negative charge of polysaccharide is reduced to values slightly less or around the optimum charge, it is noticed that the configuration of α_{s1} -casein

becomes highly distorted. Normally α_{s1} -casein on its own adopts a conformation that has been likened to those seen for adsorbed synthetic tri-block co-polymers. These have their two ends lying flat on surface and the middle section tends to extend away into the solution, forming a loop.^{46, 49-51} It is found that in the presence of the polysaccharides with charge densities close to the optimal value, the central loop section of α_{s1} -casein becomes suppressed as it is pushed towards the surface. We suspect that this is due to presence of excluded volume interactions between the hydrophilic part of the protein and the polysaccharide chains. This excluded volume interaction is strongest when the surface coverage by polysaccharide is high, i.e. at or around the optimum charge. At this same charge, the polysaccharide chains themselves are seen to be more extended. Therefore, for these systems, the structure of the interfacial layer begins to resemble that of a multi-layer. However, having said that, the equilibrium multi-layers in our work were far more evident in systems with polysaccharide molecules having a heterogeneous distribution of charge groups.

Unlike proteins, the structural diversity and range of polydispersity of food polysaccharides makes their characterization rather complicated. Nevertheless, what is clear is that many charge polysaccharides have a non-uniform distribution of charge groups along their backbone, with electric charge concentrated in small sections of the molecule. To mimic such a heterogeneous distribution of charge we have chosen the simplest possible model: a diblock structure consisting of a short part (the A-block) and a longer section (the B-block). We explored the changing adsorption pattern of the protein + polysaccharide, by redistributed the charge of the polysaccharide molecules in different ways between the A and B monomers. One can either keep the charge of the whole molecule fixed while assigning increasing portion of it to A-block, or alternatively can keep the charge of A or B monomers constant, while varying the charge of the other section. The overall conclusions that emerge from such calculations can be summarised as follows. When the difference between the charge densities of the long and short blocks is not all that great ($Z_A/Z_B < 10$), the adsorption behaviour and the structure of the interfacial layer are found to be similar to those in systems involving uniformly charged polymers. The same is also true for cases where the negative charge of B monomers is stronger than A, $|Z_B| \geq |Z_A|$. The real change in the behaviour arises when the reverse situation, $|Z_A| \gg |Z_B|$, is considered. Now we find that the long B-blocks begin to extend away from the surface, allowing for a larger number of A-blocks to be absorbed in and onto the protein layer in their place. This of course also implies a greater number of adsorbed polysaccharide molecules. The conformation adopted by these non-uniformly charged chains becomes increasingly "brush" like, as the charge on B monomers is reduced. Eventually the structure of the interfacial film resembles a multi-layer with an inner layer consisting mainly of protein, and a secondary layer made up entirely of the long weakly charged B-blocks of polysaccharide. The film is also found to be much thicker as a result. The amount of polysaccharide accumulating at the surface is now controlled by the charge of the short A-blocks. Once again we obtain a peak for the number of adsorbed chains at some optimal charge density, but now for that of A-blocks rather than the whole

polymer. It has been thought that formation of such multilayers is only possible when sufficiently strong short range interactions exist between the two sets of adsorbing polyelectrolytes.⁴² These conclusions have been obtained on the bases of uniformly charged chains. However, we have shown here that this may not need to be the case where the distribution of charge is appropriately non-uniform.

An important observation during the application of layer by layer deposition technique is the reversal of the surface potential at each stage of the process. For example, it has been found experimentally, that the adsorption of negatively charged polysaccharide onto the positively charged protein layer continues beyond the neutral point, resulting in a negative surface. Indeed, it is this reversal of surface potential that allows the construction of multi-layers by sequential adsorption of alternating charged polymers. We have studied the phenomenon of charge reversal in relation to non-homogeneity of polysaccharide charge distribution, using our SCF calculations. Our results reveal that for very low or uncharged B monomers, we have a thick extended secondary layer. But being made up of B-blocks, this layer does not contribute sufficient charge to be able to reverse the electrical potential of the surface. At the other limit, where Z_B is not that different to Z_A , the polysaccharide chains lie flat on the surface and we have a thin mixed protein + polysaccharide film. In such a system also, we do not see a significant reversal of the surface potential. However, in some intermediate values of Z_B between the two limits above, the secondary polysaccharide layer, consisting of B monomers, is observed to be reasonably thick and yet also has a sufficient amount of negative charge. Here one finds that the surface potential viewed from the bulk side is seen to be negative. While we do not underestimate the simplicity of our model, it nevertheless serves to show how non-uniform distribution of polysaccharide molecules may lead to reversed negative surface potentials of a few tens of mV, much as seen experimentally.^{29, 30, 53, 61} Thus, we believe that while not being the sole contributor, the heterogeneity of charge distribution of polysaccharide molecules is one of the important factors, hitherto not taken into account in theories that attempt to explain the phenomenon of charge reversal.

Recent experimental work by Lutz et al⁶³ considered the stability and surface potential of W/O/W double emulsions stabilised by complexes of pectin and whey protein. Transport of water from primary water emulsions to the continuous water phase was also studied. They compared a number of different pectin chains having varying degree of charge blockiness. It was found that while the most uniform pectin had the highest charge, its adsorption together with the whey protein onto the surface of the emulsion droplets actually led to a lower negative surface potential. The measured ζ -potential values were most negative for the more non-uniformly charged pectin molecules, despite their lower overall charge. The main conclusions of our calculations seem to explain this somewhat paradoxical observation rather well. Furthermore, Lutz et al⁶³ found a higher degree of colloidal stability for the emulsions stabilised by whey protein together with non-uniformly charged pectins, which they attributed in parts to the more negative surface potential of the emulsion droplets for such systems. However, the higher stability

can also indicate a more extended interfacial layer and a stronger steric repulsion, which is again predicted by our results. Additionally, Lutz et al⁶³ also found that transport of water, from primary water emulsion droplets to the continuous water phase, was slower for the uniformly charged pectin systems than that for the non-uniformly charged chains. This was believed to be due to a higher packing efficiency and a more compacted interfacial layer that hindered the transport of water molecules. Once again this is the trend we observe in our data.

We welcome MD simulation studies that consider the influence of heterogeneity of polyelectrolyte charge distribution as well as experimental studies, such as neutron reflectivity, that probe the changes in the structure of protein + polysaccharide layers more directly as such films age. However, we acknowledge that systematic experimental studies of this kind are more likely to involve well characterized synthetic polyelectrolytes, rather than natural polysaccharides.

Acknowledgment.

AA thanks ICI plc for their financial support. We also acknowledged many useful discussions with E. Dickinson.

Notes and references

Food Science and Nutrition, University of Leeds, LS2 9JT Leeds, United Kingdom. E-mail: R.Ettelaie@food.leeds.ac.uk

1. G. Decher, *Science*, 1997, **277**, 1232-1237.
2. M. Schonhoff, *Curr. Opin. Colloid Interface Sci.*, 2003, **8**, 86-95.
3. Y. H. Hong and D. J. McClements, *Food Biophysics*, 2007, **2**, 46-55.
4. Y. X. Jia, W. Han, G. X. Xiong and W. S. Yang, *Journal of Colloid and Interface Science*, 2008, **323**, 326-331.
5. Y. Lvov, K. Ariga, M. Onda, I. Ichinose and T. Kunitake, *Colloids and Surfaces a-Physicochemical and Engineering Aspects*, 1999, **146**, 337-346.
6. Y. Lvov, R. Price, B. Gaber and I. Ichinose, *Colloids and Surfaces a-Physicochemical and Engineering Aspects*, 2002, **198**, 375-382.
7. K. T. Nam, D. W. Kim, P. J. Yoo, C. Y. Chiang, N. Meethong, P. T. Hammond, Y. M. Chiang and A. M. Belcher, *Science*, 2006, **312**, 885-888.
8. K. Hyde, M. Rusa and J. Hinestroza, *Nanotechnology*, 2005, **16**, S422-S428.
9. S. Ivanov, F. Kurniawan, V. Tsakova and V. M. Mirsky, *Macromolecular Materials and Engineering*, 2009, **294**, 441-444.
10. S. Yilmazturk, H. Deligoz, M. Yilmazoglu, H. Damyan, F. Oksuzomer, S. N. Koc, A. Durmus and M. A. Gurkaynak, *Journal of Power Sources*, 2010, **195**, 703-709.
11. J. J. Ramsden, Y. M. Lvov and G. Decher, *Thin Solid Films*, 1995, **254**, 246-251.
12. A. Agarwal, T. L. Weis, M. J. Schurr, N. G. Faith, C. J. Czuprynski, J. F. McAnulty, C. J. Murphy and N. L. Abbott, *Biomaterials*, 2010, **31**, 680-690.
13. Q. W. Tang, Q. H. Li, J. M. Lin, S. J. Fan, D. Hu and J. H. Wu, *Polymer Composites*, 2010, **31**, 145-151.
14. P. Podsiadlo, M. Qin, M. Cuddihy, J. Zhu, K. Critchley, E. Kheng, A. K. Kaushik, Y. Qi, H. S. Kim, S. T. Noh, E. M. Arruda, A. M. Waas and N. A. Kotov, *Langmuir*, 2009, **25**, 14093-14099.
15. J. Kochan, T. Wintgens, J. E. Wong and T. Melin, *Desalination*, 2010, **250**, 1008-1010.
16. M. Du, T. Yang, Y. C. Zhang and K. Jiao, *Electroanalysis*, 2009, **21**, 2521-2526.
17. J. L. Lutkenhaus and P. T. Hammond, *Soft Matter*, 2007, **3**, 804-816.
18. J. A. Jaber and J. B. Schlenoff, *Curr. Opin. Colloid Interface Sci.*, 2006, **11**, 324-329.
19. A. P. R. Johnston, C. Cortez, A. S. Angelatos and F. Caruso, *Curr. Opin. Colloid Interface Sci.*, 2006, **11**, 203-209.
20. K. C. Wood, J. Q. Boedicker, D. M. Lynn and P. T. Hammond, *Langmuir*, 2005, **21**, 1603-1609.
21. M. Macdonald, N. M. Rodriguez, R. Smith and P. T. Hammond, *Journal of Controlled Release*, 2008, **131**, 228-234.
22. B. S. Kim, S. W. Park and P. T. Hammond, *ACS Nano*, 2008, **2**, 386-392.
23. U. Manna and S. Patil, *Langmuir*, 2009, **25**, 10515-10522.
24. F. Caruso, D. Trau, H. Mohwald and R. Renneberg, *Langmuir*, 2000, **16**, 1485-1488.
25. E. Dickinson, *Soft Matter*, 2008, **4**, 932-942.
26. D. J. McClements, *Biotechnology Advances*, 2006, **24**, 621-625.
27. D. Guzey and D. J. McClements, *Advances in Colloid and Interface Science*, 2006, **128**, 227-248.
28. D. Guzey and D. J. McClements, *Food Biophysics*, 2006, **1**, 30-40.
29. D. Guzey and D. J. McClements, *Journal of Agricultural and Food Chemistry*, 2007, **55**, 475-485.
30. L. Jourdain, M. E. Leser, C. Schmitt, M. Michel and E. Dickinson, *Food Hydrocolloids*, 2008, **22**, 647-659.
31. M. Beysseriat, E. A. Decker and D. J. McClements, *Food Hydrocolloids*, 2006, **20**, 800-809.
32. E. Dickinson, *Colloids Surf B Biointerfaces*, 2010, **81**, 130-140.
33. E. Dickinson, *An Introduction to Food Colloid*, Oxford University Press, 1992.
34. A. Akinchina and P. Linse, *Macromolecules*, 2002, **35**, 5183-5193.
35. A. Akinchina and P. Linse, *Journal of Physical Chemistry B*, 2003, **107**, 8011-8021.
36. C. L. Cooper, P. L. Dubin, A. B. Kayitmazer and S. Turksen, *Curr. Opin. Colloid Interface Sci.*, 2005, **10**, 52-78.
37. F. Carlsson, M. Malmsten and P. Linse, *Journal of the American Chemical Society*, 2003, **125**, 3140-3149.
38. A. V. Dobrynin, *Curr. Opin. Colloid Interface Sci.*, 2008, **13**, 376-388.
39. M. Jonsson and P. Linse, *Journal of Chemical Physics*, 2001, **115**, 3406-3418.
40. A. V. Dobrynin and M. Rubinstein, *Prog. Polym. Sci.*, 2005, **30**, 1049-1118.
41. P. A. Patel, J. Jeon, P. T. Mather and A. V. Dobrynin, *Langmuir*, 2005, **21**, 6113-6122.
42. P. A. Patel, J. Jeon, P. T. Mather and A. V. Dobrynin, *Langmuir*, 2006, **22**, 9994-10002.
43. J.-M. Y. Carrillo and A. V. Dobrynin, *Langmuir : the ACS journal of surfaces and colloids*, 2012, **28**, 1531-1538.
44. J. Scheutjens and G. J. Fleer, *Journal of Physical Chemistry*, 1979, **83**, 1619-1635.
45. J. Scheutjens and G. J. Fleer, *Journal of Physical Chemistry*, 1980, **84**, 178-190.
46. E. Dickinson, D. S. Horne, V. J. Pinfield and F. A. M. Leermakers, *Journal of the Chemical Society-Faraday Transactions*, 1997, **93**, 425-432.
47. E. Dickinson, V. J. Pinfield, D. S. Horne and F. A. M. Leermakers, *Journal of the Chemical Society-Faraday Transactions*, 1997, **93**, 1785-1790.
48. F. A. M. Leermakers, P. J. Atkinson, E. Dickinson and D. S. Horne, *Journal of Colloid and Interface Science*, 1996, **178**, 681-693.
49. R. Ettelaie, A. Akinshina and E. Dickinson, *Faraday Discussions*, 2008, **139**, 161-178.
50. R. Ettelaie, A. Akinshina and E. Dickinson, *ACS symposium series*, 2009, **1007**, 46-66.
51. A. Akinshina, R. Ettelaie, E. Dickinson and G. Smyth, *Biomacromolecules*, 2008, **9**, 3188-3200.
52. P. J. Yoo, N. S. Zacharia, J. Doh, K. T. Nam, A. M. Belcher and P. T. Hammond, *ACS Nano*, 2008, **2**, 561-571.
53. L. S. Jourdain, C. Schmitt, M. E. Leser, B. S. Murray and E. Dickinson, *Langmuir*, 2009, **25**, 10026-10037.

-
54. G. J. Fleer, M. A. Cohen Stuart, J. M. H. M. Scheutjens, T. Cosgrove and B. Vincent, *Polymers at interfaces*, Chapman and Hall, London, 1993.
55. J. Scheutjens and G. J. Fleer, *Macromolecules*, 1985, **18**, 1882-1900.
- 5 56. O. A. Evers, J. Scheutjens and G. J. Fleer, *Macromolecules*, 1990, **23**, 5221-5233.
57. M. R. Bohmer, O. A. Evers and J. Scheutjens, *Macromolecules*, 1990, **23**, 2288-2301.
58. R. Israels, J. Scheutjens and G. J. Fleer, *Macromolecules*, 1993, **26**,
10 5405-5413.
59. R. Israels, F. A. M. Leermakers and G. J. Fleer, *Macromolecules*, 1994, **27**, 3087-3093.
60. R. J. Hunter, *Foundations of Colloid Science*, Clarendon Press, Oxford, 2000.
- 15 61. M. T. Sejersen, T. Salomonsen, R. Ipsen, R. Clark, C. Rolin and S. B. Engelsen, *International Dairy Journal*, 2007, **17**, 302-307.
62. E. B. Zhulina and F. A. M. Leermakers, *Soft Matter*, 2009, **5**, 2836-2840.
63. R. Lutz, A. Aserin, L. Wicker and N. Garti, *Colloid Surf. B-Biointerfaces*, 2009, **72**, 121-127.
20

25

Figure Captions

Fig. 1 Illustration of homopolymer A_{500} and diblock $A_{20}B_{480}$ models of polysaccharides.

Fig. 2 Adsorbed amount of protein and polysaccharide as a function of polysaccharide segment charge (absolute value in units of e). The surface coverage data are given in units of equivalent saturated monolayers.

Fig. 3 Volume fraction profiles of adsorbed α_{S1} -casein and uniformly charged polysaccharide, for three different cases with varying polysaccharide charge density, Z_A . Dashed lines (a,b,c) show volume fraction of the protein, solid lines (d,e,f) are for the polysaccharide. The values of the charge density are: a and d, $Z_A = -0.0496e$; b and e, $Z_A = -0.1e$; c and f, $Z_A = -1.0e$.

Fig. 4 Average distance from the surface for individual monomers of (a) α_{S1} -casein and (b) homopolymer polysaccharide, at different polysaccharide monomer charge: a, $Z_A = -0.0496e$; b, $Z_A = -0.1e$; c, $Z_A = -1.0e$.

Fig. 5 Adsorbed amount of protein and polysaccharide plotted as a function of absolute charge of A-segment of the diblock polysaccharide.

Fig. 6 Volume fraction profiles of uniformly charged homopolymer (bold line a, $Z_A = -0.0496e$) and diblock polysaccharide $A_{20}B_{480}$ with different re-distribution of charge between the blocks. The charge ratios Z_A/Z_B are: b, $-0.52/-0.03$; c, $-0.7/-0.0225$; d, $-1.0/-0.01$; e, $-1.24/0$. The total charge of the polysaccharide is kept constant at $Z_{tot} = -24.8e$ for all cases. The volume fraction of the protein for system (e) is also included (dashed line) and remains almost the same for all other cases.

Fig. 7 Average distance from the surface for each monomer along the backbone of a uniformly charged homopolymer (bold line a, $Z_A = -0.0496e$) and diblock polysaccharide $A_{20}B_{480}$ with different charges on A and B blocks. The charge distributions Z_A/Z_B are: b, $-0.52/-0.03$; c, $-0.7/-0.0225$; d, $-1.0/-0.01$; and e, $-1.24/0$.

Fig. 8 Adsorbed amount of protein and polysaccharide as a function of (a) absolute charge of A-segments ($|Z_A|$) of the diblock polysaccharide (with $Z_B = -0.01e$), (b) absolute charge of B-segments ($|Z_B|$) of the diblock polysaccharide (with $Z_A = -1.0e$).

Fig. 9 Volume fraction profiles for the model diblock polysaccharide. Figure (a) shows different charge of A-monomers: a, -0.25 ; b, -0.5 , c, -1.0 ; d, -3.0 ($Z_B = -0.01$) and figure (b) shows different charge of B-monomers: a, -0.01 ; b, -0.03 , c, -0.05 ; d, -0.1 ($Z_A = -1.0$).

Fig. 10 Average distance from the surface plotted against the ranking along the backbone for individual monomers of the diblock polysaccharide model. Graph (a) is for varying charge of A-monomers: a, -0.25 ; b, -0.5 , c, -1.0 ; d, -3.0 ($Z_B = -0.01e$) and graph (b) is for varying charge of B-monomers: a, $-0.01e$; b, $-0.03e$, c, $-0.05e$; d, $-0.1e$ ($Z_A = -1.0e$).

Fig. 11 Variation of the electrostatic potential, $\Psi_{el}(r)$, versus distance away from the surface, r , for polysaccharide adsorbed onto the α_{S1} -casein layer. In set of graphs (a) polysaccharide is uniformly charged (A_{500}) with charge densities, Z_A : a (bold), $-0.0496e$; b, $-0.1e$; c, $-0.3e$; d, $-0.5e$; e, $-1.0e$. In graphs (b) polysaccharide has a $A_{20}B_{480}$ structure, with a fixed total charge $Z_{tot} = -24.8e$ for all cases, and varied charge distributions Z_A/Z_B along the chain: a, (bold, homopolymer) $-0.0496/-0.0496$; b, $-0.52/-0.03$; c, $-1.0/-0.01$; d, $-1.12/-0.005$; and e, $-1.24/0$. Set of graphs (c) are the same as (b) but now keeping $Z_B = -0.01e$, while Z_A is varied: a, $-0.25e$; b, $-0.5e$, c, $-1.0e$; d, $-3.0e$, and for graphs (d) Z_A is kept constant at $-1.0e$, while Z_B is changing: a, $-0.005e$; b, $-0.01e$, c, $-0.03e$; d, $-0.05e$; and e, $-0.1e$. The dashed line in set of graphs (a) indicates the electrostatic potential in absence of polysaccharide (protein layer only).

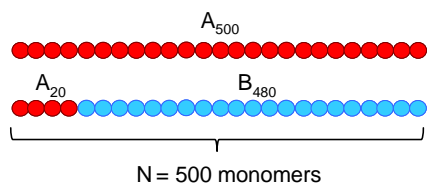
5 **FIGURE 1**

10

15

Homopolymer

20
Diblock



25

FIGURE 2

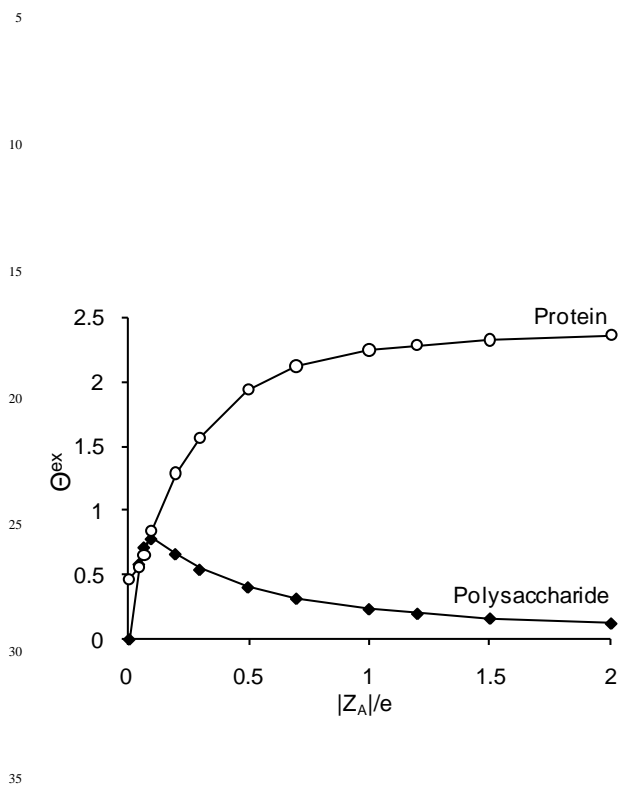
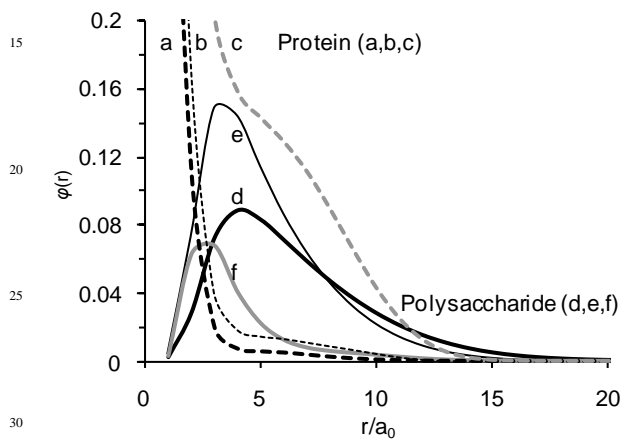


FIGURE 3

5

10



35

FIGURE 4

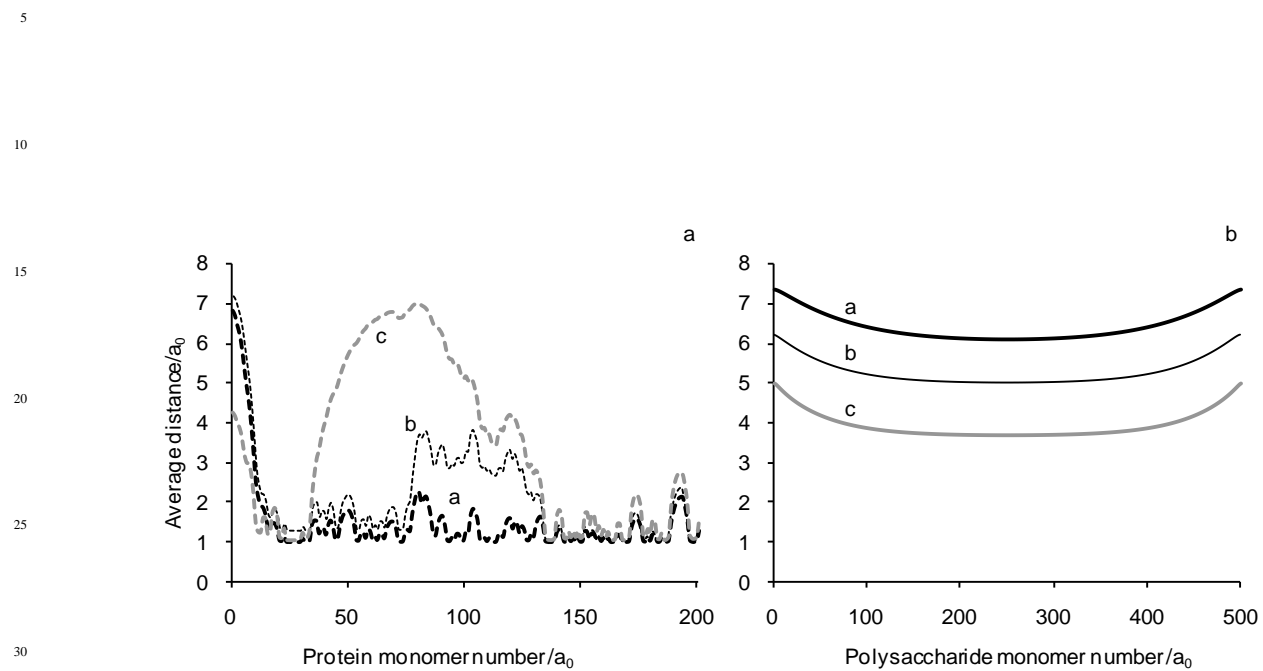


FIGURE 5

5

10

15

20

25

30

35

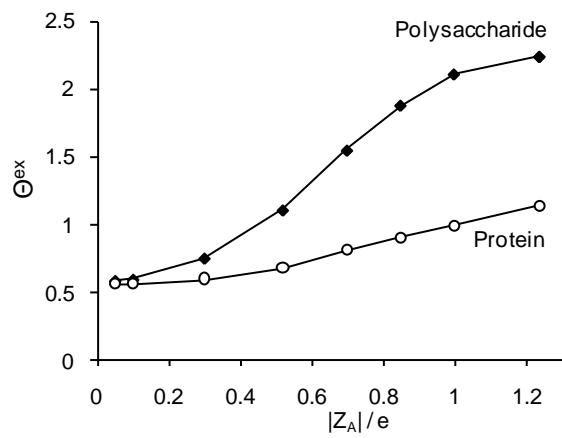


FIGURE 6

5

10

15

20

25

30

35

40

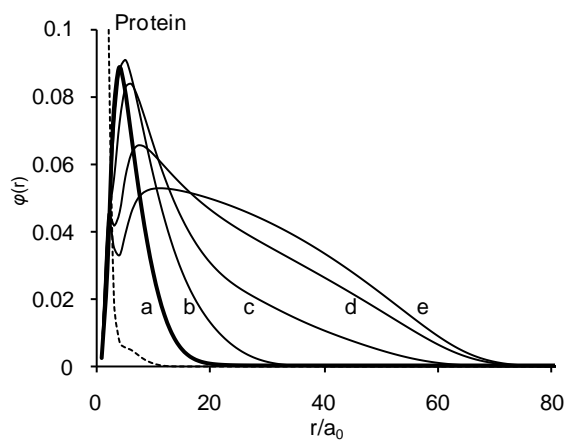


FIGURE 7

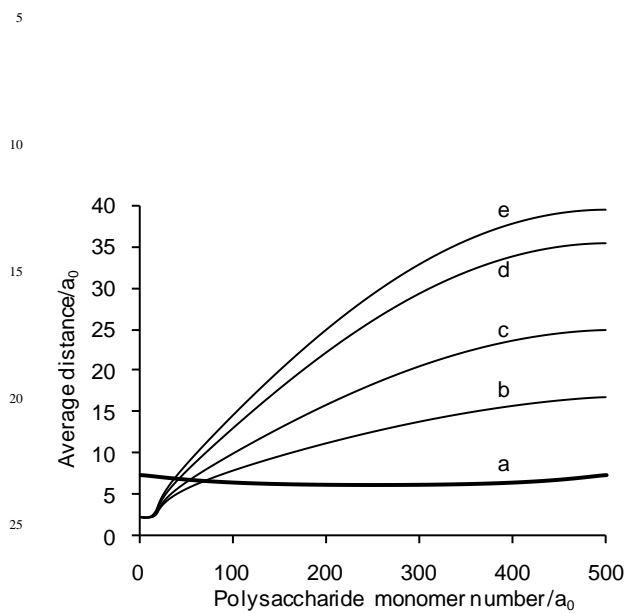


FIGURE 8

5

10

15

20

25

30

35

40

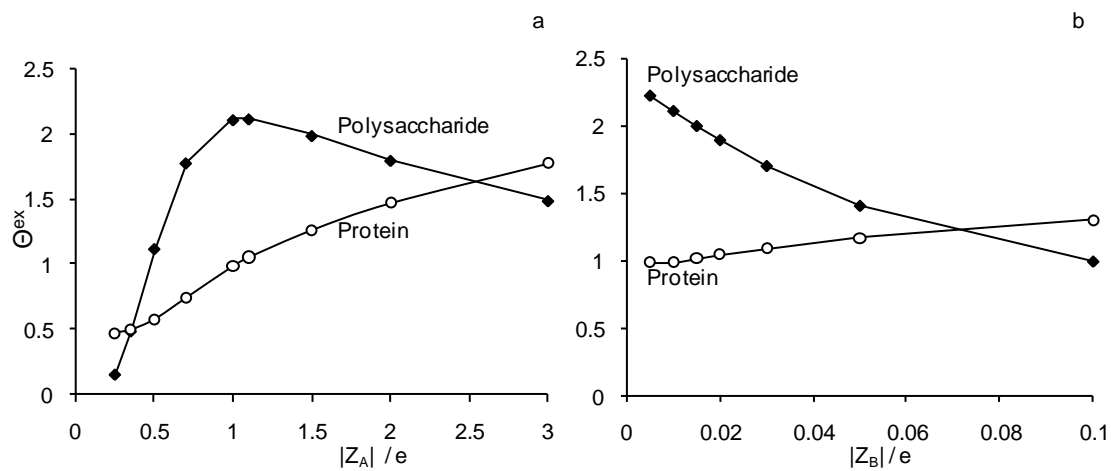


FIGURE 9

5

10

15

20

25

30

35

40

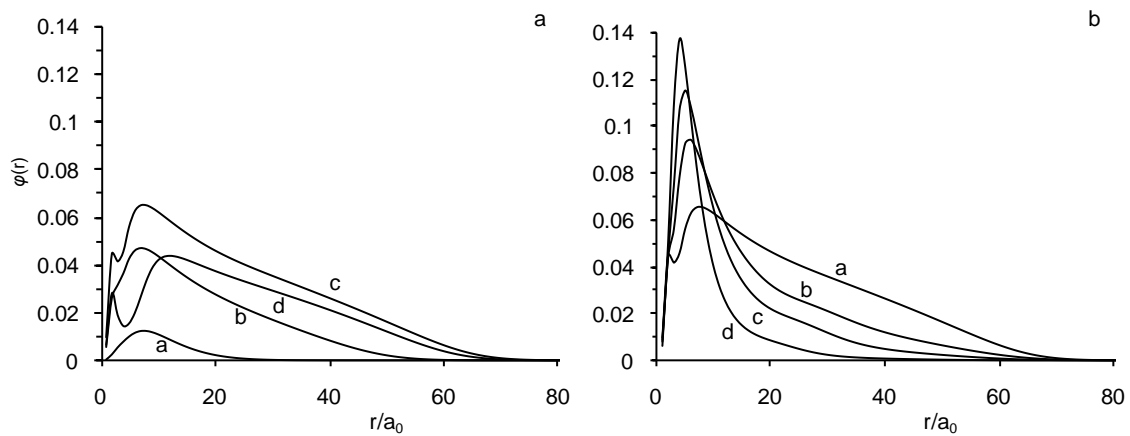


FIGURE 10

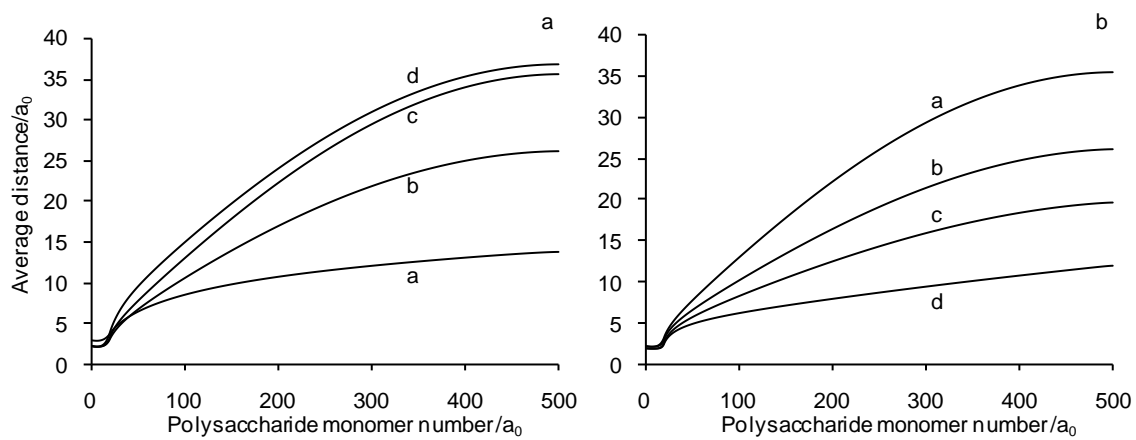


FIGURE 11

5

10

15

20

25

30

35

40

45

50

55

60

65

